Electronic Supplementary Material (ESI) for Journal of Materials Chemistry C.

Supplemental Material

Electrical switching of magnetization in a layer of α-Fe with naturally hydroxidized surface

N.I. Polushkin,[1,2,5] A.C. Duarte,[1,2] O. Conde,[1,2] N. Bundaleski,[3] C. Dias,[4] J.O. Ventura,[4] J.P. Araujo,[4] G.N. Kakazei,[4] P. Lupo,[5] A.O. Adeyeye,[5] S. Cardoso[6]

[1]*Departamento de Física, Faculdade de Ciências, Universidade de Lisboa, 1749-016 Lisboa, Portugal*
[2]*CeFEMA-Center of Physics and Engineering of Advanced Materials. 1049-001 Lisboa. Portugal*
[3]*Vinča Institute of Nuclear Sciences, University of Belgrade, P.O. Box 522 11001, Serbia*
[4]*University of Porto, Department of Physics and IFIMUP, 4169-007 Porto, Portugal*
[5]*Electrical & Computer Engineering, National University of Singapore, 17583 Singapore*
[6]*INESC MN, 1000-029 Lisbon, Portugal*

I. MICROSTRUCTURAL STUDIES

Figure **S1 (a-b)** shows a SAED pattern for a Si(100)/α-Fe sample prepared by PLD at P_0=1.0×10^{-6} mbar, where we mark up to four diffraction rings – with the ratios between their radiuses consistent to the inverse values of the interplanar distances in α-Fe. Figure **S1 (c-d)** illustrates GIXRD data collected for the same sample in two geometries: The x-ray incidence plane is parallel to either the (110) or (100) plane. As seen, in the GIXRD pattern taken under these configurations there are two discerned peaks. One of them arises at 2θ≈44.5° to be attributed to a (110) reflection of α-Fe. Its full width at half of maximum is about $2\Delta\theta_{0.5}$≈4.5°, so that the averaged grain diameter in the α-Fe evaluated according to the Scherrer equation is ~4.0 nm. Another peak appears to be at 2θ≈27.5°. Among all known iron oxides and hydroxides, there are three oxyhydroxide polymorphs, notably γ-FeOOH (lepidocrocite), β-FeOOH (akageneite), and high-pressure (hp) FeOOH, that give relatively strong reflections at this angle [**S1**]. All of these phases are known [**S1**] to be antiferromagnetic in bulk – with Néel temperatures of 77 K, 290 K , and 470 K, respectively. As the GIXRD patterns indicate the presence, at least, of the two phases, contrary to the SAED data that reveal α-Fe only, the GIXRD data confirm the formation of the bilayer structure, i.e., the α-Fe layer covered by the surface layer which is enriched with the FeOOH polymorph(s). The atomic structure of one of them, γ-FeOOH, whose contribution to the chemical composition of corroded surfaces of iron and steels is more detectable [**S2**, **S3**], is presented in Fig. **S2**. In its bulk form γ-FeOOH is an insulator (band gap is ~2.06 eV) and electric conductivity of ~10^{-7} Ω^{-1}m^{-1} [**S1**]. It is also important that there are no any significant changes in the GIXRD peak originating from the FeOOH phase after thermal annealing up to 400C.

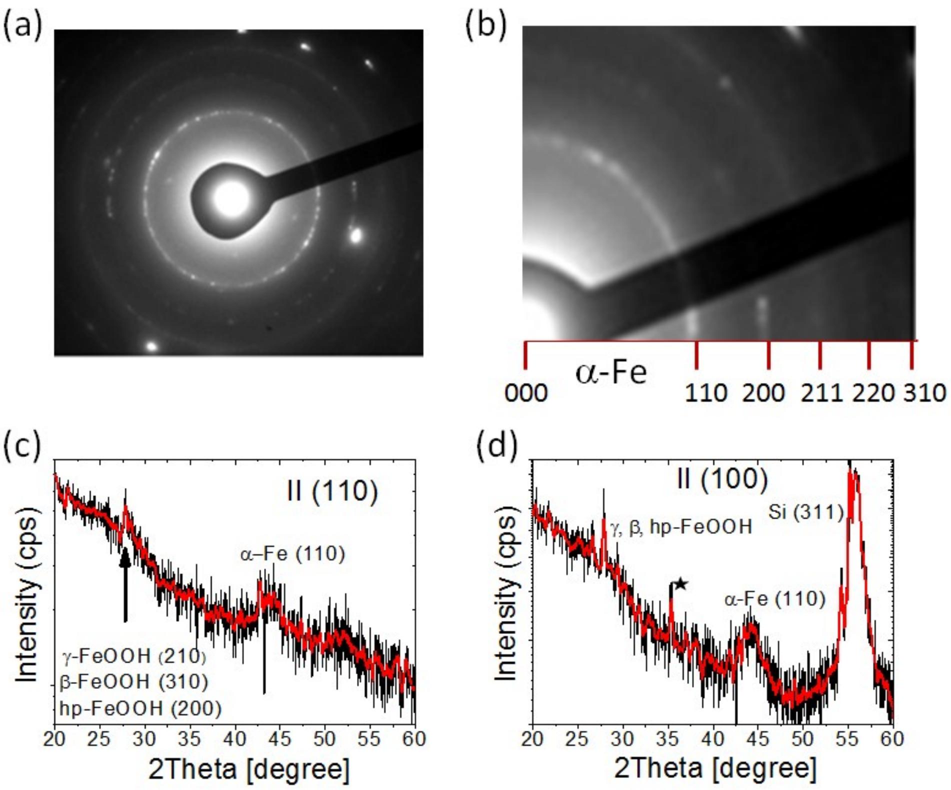

Fig. S1. (a) Electron diffraction pattern (SAED) taken in the transmission mode (TEM) for a sample prepared by PLD at P_0=1.0×10^{-6} mbar. **(b)** A quarter of the same SAED pattern that is shown in **(a).** There is good agreement with inverse planar distances of α-Fe. **(c-d)** GIXRD patterns taken at a 2-degree grazing angle and the two orientations of the x-ray incidence plane with respect to the sample. The two discerned peaks respectively indicate the presence of the oxyhydroxide phase(s) – γ-FeOOH, β-FeOOH, and/or hp-FeOOH – at 2θ~27.5° [**S1**] and α-Fe at 2θ~44.5°. A 'star' symbol in the pattern taken under the II (100) geometry **(d)** indicates a spurious peak.

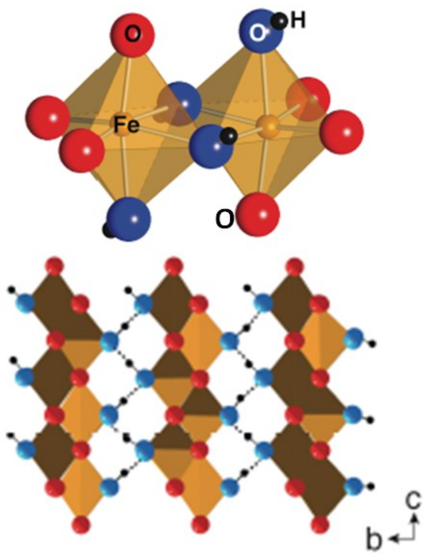

Fig. S2. Top: The double chain formed by two edging sharing $FeO_3(OH)_3$ octaedra which are building units common for all ferric oxides and hydroxides. Bottom: Stacking of sheets in γ-FeOOH with the double chains of Fe-octaedra running parallel to the **c** axis. The sheets are held together by hydrogen bonds [**S4**]. The parameters of the γ-FeOOH unit cell are as follows: *a*=0.307 nm, *b*=1.252 nm, *c*=0.387 nm.

II. CIMS TEST WITH VSM

In addition to controlling *in situ* the CIMS process with MOKE, we verified it *ex situ* with a Lake Shore vibrating sample magnetometer (VSM) system. For the latter test, we have used a high-P_0 sample having lateral sizes $L \approx 3.0 \times 3.0$ mm^2. The sample was preliminarily magnetized along the film plane with a field B=100 mT up to saturation, as indicated in Fig.**S3(a)**. This procedure was controlled with the VSM system. Then, the sample was mounted in the CIMS setup [Fig. **1(a)]** for discharging a capacitor C=5.0 μF through it with no a biasing field (B=0) at the interpad gap S close to L and U=+50 V [Fig. **S3(b)**]. According to the CIMS data illustrated in Fig.**2**, these parameters were sufficient for the switching. At the next step, the sample was mounted again into the VSM system for measuring its magnetization state in an external magnetic field applied in the same direction and sweeping from zero to +10 mT and back (shown by arrows). We find that the magnetic moment has changed its sign after CIMS [Fig.**S3(c)**]. This experiment provides straightforward evidence for switching of magnetization under discharging a capacitor.

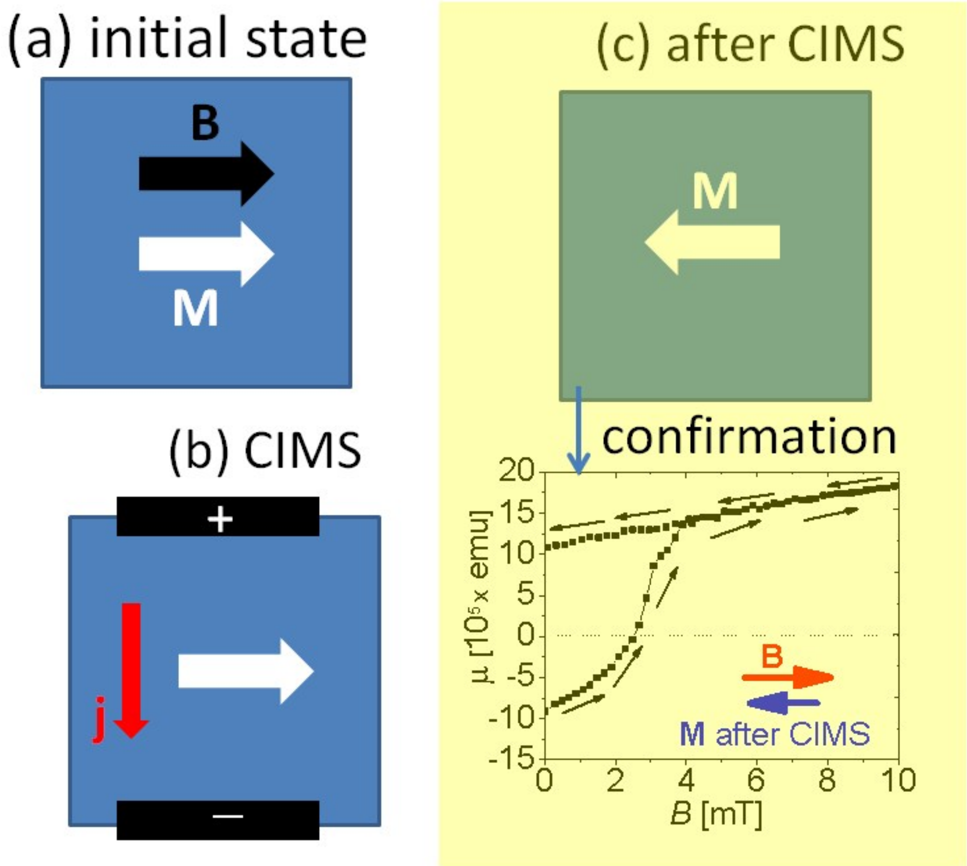

Fig.S3. VSM test for CIMS: **(a)** A sample is magnetized with a field B up to saturation – with controlling by VSM (not shown); **(b)** CIMS procedure; **(c)** The CIMS effect is confirmed with VSM.

III. OERSTED FIELD CALCULATION

The magnetic field **B** generated by an electric current **j** flowing through a conductor in the three-dimensional space is given by the following magnetostatics equation:

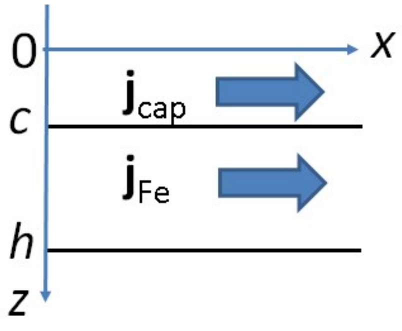

Fig. S4. Coordinate system and schematic for the calculation of the Oersted field

$$\mathbf{curl\ B} = \mu_0 \mathbf{j}. \quad \text{(S1)}$$

To solve Eq. (S1), one uses the vector potential **A** that satisfies the condition div **A**=0 and is defined as

$$\mathbf{B} = \mathbf{curl\ A}, \quad \text{(S2)}$$

From Eqs. (S1) and (S2) – with taking into account that

$\mathbf{curl\ curl\ A} = \mathbf{grad}\ \mathrm{div}\ \mathbf{A} - \Delta\mathbf{A} = -\Delta\mathbf{A}$ – one gets that

$$\Delta\mathbf{A} = -\mu_0 \mathbf{j}. \quad \text{(S3)}$$

For a current flowing along the x axis through a thin plate infinite in the x-y plane, Eq. (S3) is reduced to the following one [**S5**]

$$\frac{\partial^2 A_x}{\partial z^2} = -\mu_0 j_x\,, \quad \text{(S4)}$$

so that in the infinite geometry there is only a one component of the Oersted field, $B_y = \partial A_x / \partial z$. With neglecting interfacial currents, B_y should be continuous across an interface

$$\left.\frac{\partial A_x}{\partial z}\right|_{+} = \left.\frac{\partial A_x}{\partial z}\right|_{-} \quad \text{(S5)}$$

For the two-layer system of a ferromagnetic (Fe) film with capping, as schematically illustrated in Fig. **S4**, the magnetic field, generated by the currents flowing along the x axis through both Fe (j_{Fe}) and cap (j_{cap}), is given as superposition of the fields $B_{y,\text{Fe}}$ and $B_{y,\text{cap}}$ generated separately by j_{Fe} and j_{cap}

$$B_y = B_{y,\text{Fe}} + B_{y,\text{cap}} \quad \text{(S6)}$$

We will calculate separately these two partial fields and then find their sum. For an Fe layer, the system of equations and boundary conditions are as follows:

$$\frac{\partial^2 A_{z<c}}{\partial z^2} = 0; z < c$$
$$\frac{\partial^2 A_{\text{Fe}}}{\partial z^2} = -\mu_0 j_{\text{Fe}}; c < z < h \tag{S7}$$
$$\frac{\partial^2 A_{z>h}}{\partial z^2} = 0; z > h$$

$$\begin{aligned} \partial A_{z<c}/\partial z\big|_{z=c} &= \partial A_{\text{Fe}}/\partial z\big|_{z=c} \\ \partial A_{\text{Fe}}/\partial z\big|_{z=h} &= \partial A_{z>h}/\partial z\big|_{z=h} \end{aligned} \tag{S8}$$

By integrating Eqs. (S7) one gets that

$$\frac{\partial A_{z<c}}{\partial z} = C_1$$
$$\frac{\partial A_{\text{Fe}}}{\partial z} = -\mu_0 j_{\text{Fe}} z + C_2 \tag{S9}$$
$$\frac{\partial A_{z>h}}{\partial z} = C_3$$

Using the boundary conditions (S8), one obtains from (S9) that

$$\begin{aligned} C_1 &= -\mu_0 j_{\text{Fe}} c + C_2 \\ C_3 &= -\mu_0 j_{\text{Fe}} h + C_2 \end{aligned} \tag{S10}$$

Because of the symmetry of the system

$$|C_1| = |C_3| \ . \tag{S11}$$

Therefore, from (S10) one gets that

$C_1 = -C_3$, i.e., $-\mu_0 j_{\text{Fe}} c + C_2 = \mu_0 j_{\text{Fe}} h - C_2$, and finally

$$\begin{aligned} C_2 &= \frac{\mu_0 j_{\text{Fe}}(h+c)}{2} \\ C_1 &= \frac{\mu_0 j_{\text{Fe}}(h-c)}{2} \end{aligned} \tag{S12}$$

Then, the magnetic field generated by j_{Fe} is given by

$$B_{y,\text{Fe}} = \begin{cases} \frac{\mu_0 j_{\text{Fe}}}{2}(h-c); z < c \\ \frac{\mu_0 j_{\text{Fe}}}{2}(-2z+h+c); c < z < h \\ -\frac{\mu_0 j_{\text{Fe}}}{2}(h-c); z > h \end{cases} \tag{S13}$$

Replacing c by 0 and h by c in (S13), we get for the magnetic field generated by a current in the cap, j_{cap}

$$B_{y,\text{cap}} = \begin{cases} \frac{\mu_0 j_{\text{cap}}}{2} c; z < 0 \\ \frac{\mu_0 j_{\text{cap}}}{2}(-2z + c); 0 < z < c \\ -\frac{\mu_0 j_{\text{cap}}}{2} c; z > c \end{cases} \tag{S14}$$

Finally, we get the total field as superposition of these two partial fields

$$B_y = \begin{cases} \frac{\mu_0 j_{\text{cap}} c}{2}(1 + \frac{1}{\eta}\frac{h-c}{c}); z < 0 \\ \frac{\mu_0 j_{\text{cap}} c}{2}(\frac{c-2z}{c} + \frac{1}{\eta}\frac{h-c}{c}); 0 < z < c \\ \frac{\mu_0 j_{\text{cap}} c}{2}(-1 + \frac{1}{\eta}\frac{h+c-2z}{c}); c < z < h \\ -\frac{\mu_0 j_{\text{cap}} c}{2}(1 + \frac{1}{\eta}\frac{h-c}{c}); z > h \end{cases} \tag{S15}$$

where $\eta = j_{\text{cap}} / j_{\text{Fe}} = \sigma_{\text{cap}} / \sigma_{\text{Fe}}$ with σ_{Fe} and σ_{cap} being electric conductivities in Fe and its capping. If a thickness of the cap is zero (c=0), the B_{y} distribution across the Fe layer becomes strictly symmetrical woth respect to z=h/2, i.e., identical to that in a single Fe layer irrespective of the current density in in such a zero-thick capping.

IV. TEMPERATURE ELEVATION DURING A DISCHARGE

Joule heating of the material between the pads during discharging a capacitor can be calculated as [**S6**]

$$\Delta T(t) = 2\sqrt{\pi} h j^2 \exp(-2t/t_{\text{d}}) \sqrt{\mu_{\text{sub}} t} / K_{\text{sub}} / \sigma, \tag{S16}$$

where t_{d}=RC is the discharge time, h and σ the thickness and electric conductivity of the layer through which the capacitor discharges, j the density of discharge current, μ_{sub}=0.8 cm^2/s and K_{sub}=149 W/mK are respectively the heat conductivity and diffusivity of substrate. In Fig.**S5** we show the calculated temperature as a function of time (t) for discharging the capacitor through a layer of α-Fe of a thickness of h=27.0 nm and σ_{Fe}=1.0×10^7 Ω^{-1}m^{-1} (bulk α-Fe) (**a**) and through the capping (FeOOH) of a thickness of h_{cap}=6.1 nm and $\sigma_{\text{cap}}/\sigma_{\text{Fe}}$=10 at different current densities. These temperature elevations were plotted at C=5.0 μF, while the electric resistance taken was R=0.74 Ω (corresponds to bulk of α-Fe) and R=1.5 Ω (measured with two probes for the high-P_0 samples) for plotting temperature elevations in Fe and cap layers, respectively.

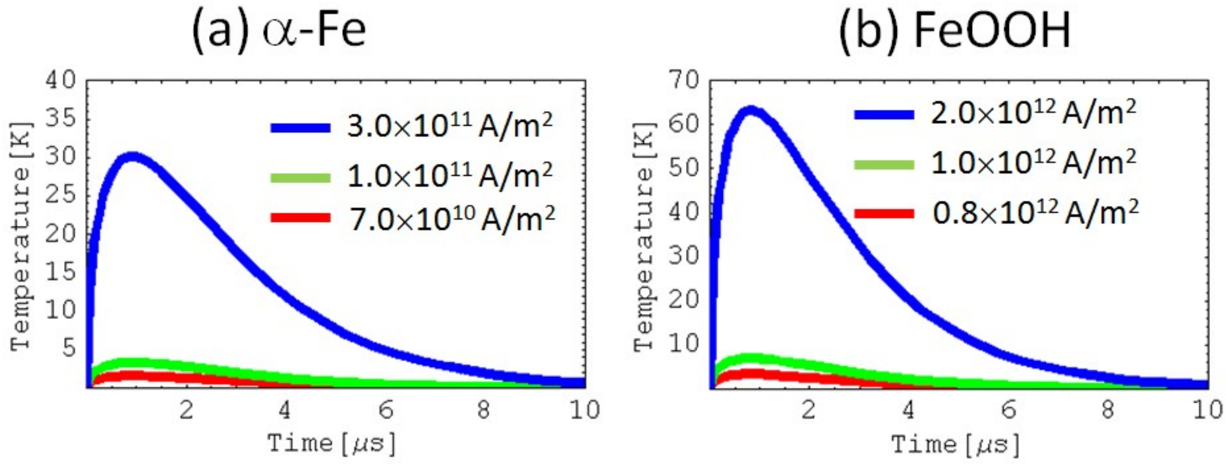

Fig.S5. Calculated temperature elevation between the pads as a function of time during discharging a capacitor C=5.0 μF through a 27-nm-thick layer of α-Fe **(a)** and through a 6-nm-thick cap layer (FeOOH) with the electric conductivity $\sigma_{cap} / \sigma_{Fe}$=10 **(b)** at different current densities.

REFERENCES

[S1] R.M. Cornell, U. Schwertmann, The Iron Oxides (Wiley-VSH Verlag GmbH & Co. KGaA, Weinheim, 2003), II Ed.

[S2] R. Balasubramaniam, A.V. Ramesh Kumar, and P. Dillmann, Characterization of rust on ancient Indian iron, *Current Science*, **85**, 1546-1555 (2003)

[S3] X.-m.Yang, Study on the infrared spectra and Raman spectra of steel rusty layer with atmospheric corrosion, *Spectroscopy and Spectral Analysis* **26**, 2247-2250 (2006)

[S4] A. P. Zhukhlistov, Crystal structure of lepidocrocite FeO(OH) from the electron-diffractometry data, *Crystallography Reports* **46**, 730–733 (2001)

[S5] L. D. Landau, E.M. Lifshitz, L. P. Pitaevskii, Electrodynamics of continuous media, II Ed. (Pergamon Press, Oxford), 1984

[S6] C.-Y. You, I. M. Sung, B.-K. Joe, Analytic expression for the temperature of the current-heated nanowire for the current-induced domain wall motion, *Appl. Phys. Lett*. **89**, 222513 (2006)